Supporting information for

A Hydrolytically Stable Anionic Layered Indium Framework for the Efficient Removal of ^{90}Sr from Seawater

Guodong Li,[‡a, b] Guoxun Ji,[‡a] Wei Liu,[‡c] Jiarong Zhang,[b] Liping Song,[b] Liwei Cheng,[b] Xia Wang,[b] Yanlong Wang,[b] Jianjun Liu,[d] Xudan Chen,[a] Xinli Sun,[a] and Juan Diwu[b]*

[a] *Xi'an Research Institute of Hi-Technology, Hong Qing Town, Xi'an 710025, Shaanxi, China.*
[b] *School for Radiological and Interdisciplinary Sciences (RAD-X) and Collaborative Innovation Center of Radiation Medicine of Jiangsu Higher Education Institutions, Soochow University, 199 Ren'ai Road, Suzhou 215123, China.*
[c] *School of Environment and Material Engineering, Yantai University, Yantai 264005, Shandong, China.*
[d] *The 986th Hospital of the People's Liberation Army Air Force. Xi'an 710054, Shaanxi, China.*

Table of Contents

Supporting information 1
S1. Chemicals and reagents 2
S2. Physical characterizations 2
S3. Crystallographic data of SZ-6 3
S4. The stability of SZ-6 4
S5. The kinetics studies 5
S6. The isotherm studies 6
S7. FT-IR spectra of SZ-6 before and after Sr^{2+} adsorption. 8
S8. EDS analysis 8
S9. X-ray photoelectron spectroscopy 9
S10. The reusability test 9
S11. The distribution coefficient K_d 9
S12. Thermodynamic Study 10
S13. The main components of seawater. 10

S1. Chemicals and reagents

All the solvents and reagents were purchased from commercial suppliers and used without further purification. 2,5-Pyridinedicarboxylic Acid ($C_7H_5NO_4$, 98%) was obtained from Shanghai Macklin Biochemical Co., Ltd. Indium(III) nitrate tetrahydrate ($In(NO_3)_3 \cdot 4H_2O$,99.99%) was purchased from Shanghai Energy Chemical, and nonradioactive strontium nitrate ($Sr(NO_3)_2$, 99%) was purchased from Shanghai Runjie Chemical Reagent Co., Ltd. Tetraethylammonium bromide ($C_4H_{12}BrN$, 98%) was purchased from J&K Scientific Co., Ltd. N,N-Dimethylformamide(DMF, AR) was received from Chinasun Specialty Products Co., Ltd. Nitric acid (HNO_3, AR, 65.0-68.0%) was purchased from Sinopharm Chemical Reagent Co., Ltd. Methanol(95%) was purchased from Shanghai Lingfeng Chemical Reagent Co., Ltd. An original stock solution of $^{90}Sr^{2+}$ with a total β activity of 10,000 counts per minute (cpm) was received and diluted to desired concentrations for further use. A real seawater sample was collected from East China Sea (pH 8.03) and filtrated to remove visible precipitates. Considering the high toxicity of ^{90}Sr, all of the adsorption experiments were carried out using the solution of nonradioactive strontium.

S2. Physical characterizations

Single crystal X-ray diffraction (SCXRD) data collections were performed on a Bruker D8-Venture diffractometer with a Turbo X-ray Source (Mo–Kα radiation, λ = 0.71073 Å), adopting the direct-drive rotating anode technique and using a CMOS detector, at 296 K. The data collections were carried out using the program APEX3 and data was processed with SAINT routine in APEX3. The crystal structures were solved with direct methods and refined by the full-matrix least squares on F^2 using the SHELXTL-2018/3 program[1]. Crystallographic information is given in Table S1 and the crystallographic file (CIF) is provided in the Supporting Information.

Powder X-ray diffraction (PXRD) data was collected from 5 ° to 50 ° with a step of 0.02°on a Bruker D8 Advance diffractometer equipped with Cu Kα radiation (λ=1.54056 Å) and an attached Lynxeye one-dimensional detector. Thermogravimetric analysis was carried out on a NETZSCH STA 449F3 instrument in the range of 30-900 ℃ under a nitrogen flow at a heating rate of 10 ℃·min^{-1}. Elemental analysis (C, N, and H) were conducted with a Vario EL CHNS elemental analyzer. Transmittance mid-Fourier transform infrared (FT-IR) measurements were carried out in the range of 4000 - 400 cm^{-1} on a Thermo Nicolet iS50 spectrometer. SEM and energy-dispersive spectroscopy (EDS) images were collected on a FEI Quanta 200FEG Scanning Electron Microscope with the energy of the electron beam of 30 keV. X-ray photoelectron spectroscopy (XPS) was

carried out on an ESCALAB 250XI X-ray Photoelectron Spectrometer Microprobe. The concentrations of Sr^{2+} in solution were measured by inductively coupled plasma-atomic emission spectrometry (ICP-OES, Thermo Fisher Scientific iCAP 7000). The radioactivity of the $^{90}Sr^{2+}$ solution was measured by a liquid scintillation counting system (LCS, Tri-Carb 2910TR). The dose rate of β-irradiation experiments is 2250 kGy/h using an electron beam (2.2 MeV) provided by an electron accelerator, while γ-irradiation experiments were conducted using a ^{60}Co irradiation source (2.22×10^{15} Bq) with a dose rate of 2.1 kGy/h.

S3. Crystallographic data of SZ-6

Table S1. Crystallographic Data and structural refinement for **SZ-6**

Formula	$C_{46}H_{30}In_3N_7O_{24}$
MM [g mol^{-1}]	1409.23
Crystal system	Trigonal
Space group	$R\bar{3}c$
a (Å)	15.7163(18)
b (Å)	15.7163(18)
c (Å)	52.205(10)
α (°)	90
β (°)	90
γ (°)	120
V (Å^3)	11167(4)
Z	6
D_c (g cm^{-3})	1.300
μ (mm^{-1})	0.986
F (000)	4164
T(K)	296(2)
R1,[a] wR2[b] ($I > 2\sigma(I)$)	0.0516, 0.1368
R1,[a] wR2[b] (all data)	0.0856, 0.1496

[a]$R_1 = \Sigma||F_o|-|F_c||/\Sigma|F_o|$. [b]$wR_2=[\Sigma w(F_o^2-F_c^2)^2/\Sigma w(F_o^2)^2]^{1/2}$

S4. The stability of SZ-6

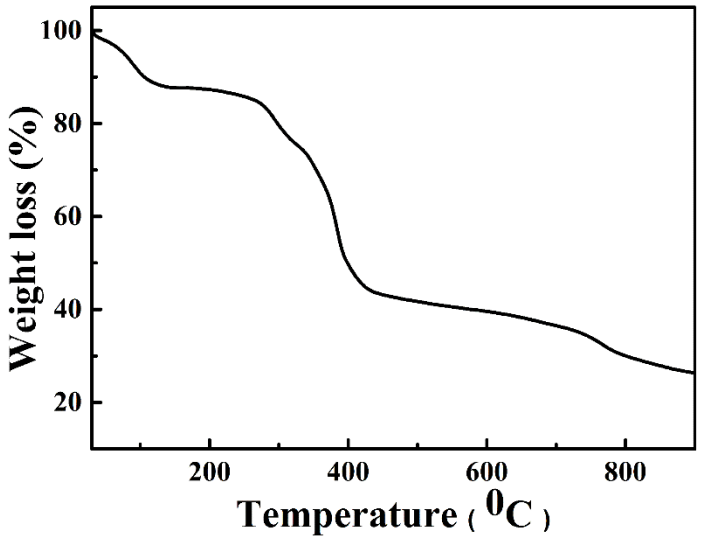

Figure S1. The thermogravimetric analysis curve of **SZ-6**.

As shown in Figure S3, the PXRD pattern of the as-synthesized material agrees well with the simulated pattern obtained from the single crystal data. There is a ca. 0.25 degree peak shift between the PXRD pattern of the as-synthesized material and the simulated one. Similar phenomenon has been reported before[2]. Such a shift in diffraction peaks indicates a uniform change in the interplanar *d*-spacing, which is generally induced by the distance variation of the adjacent layers of the structure. In this case, it is speculated that the peak shift was induced by partially exchange of the solvent molecules when the as-synthesized material was washed with ethanol.

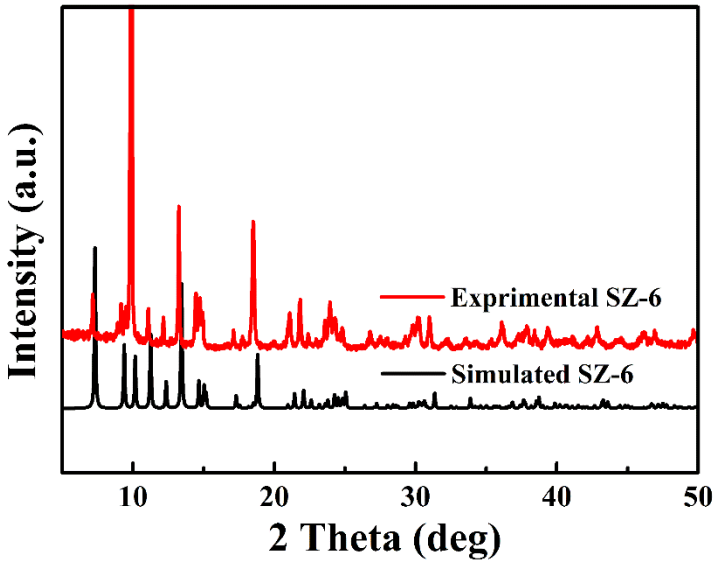

Figure S2. Powder X-ray diffraction patterns of **SZ-6**.

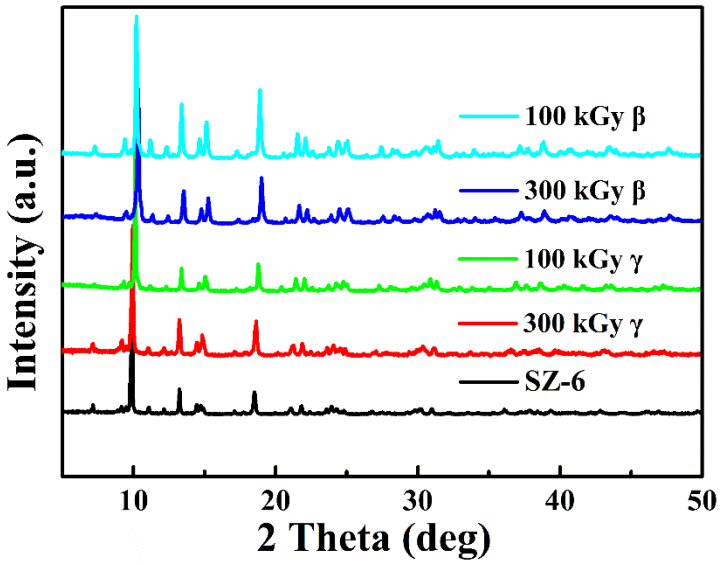

Figure S3. The PXRD patterns of **SZ-6** samples irradiated by β and γ radiation in aqueous solution.

S5. The kinetics studies

The linear form of pseudo-first-order model is expressed as:

$$\ln(q_e - q_t) = \ln q_e - k_1 t$$

where k_1 is the rate constant of pseudo-first-order adsorption (min^{-1}); t is the adsorption time (min), q_e and q_t are the adsorption capacity (mg g^{-1}) at equilibrium time and contact time t, respectively. The values of k_1 and q_e were determined from the slope and the intercept of plotting of ln (q_e-q_t) versus t.

The pseudo-second-order model was used to fit the sorption kinetics data. The model can be expressed in the following equation[3, 4]:

$$\frac{t}{q_t} = \frac{1}{k_2 q_e^2} + \frac{t}{q_e}$$

where k_2 is the rate constant of pseudo-second-order adsorption (g mg^{-1} min^{-1}). The linearized plots of pseudo-second-order model were obtained when we plotted t/q_t against t, of which the equilibrium adsorption capacity q_e and the second-order constant k_2 could be obtained from the slope and intercept.

The relationship between the amount of adsorbed ions and the square root of time indicates the effect of the intraparticle diffusion on the overall rate of ion exchange. The intra-particle diffusion equation is expressed as:

$$q_t = K_{diff} t^{1/2} + C$$

where K_{diff} is the intra-particle diffusion rate constant (mg g^{-1} min^{-1}) and C is the intercept.

Table S2. Kinetic parameters of pseudo-first-order, pseudo-second-order and Intraparticle diffusion kinetic models.

Pseudo-first-order			Pseudo-second-order			Intraparticle diffusion		
q_e(mg/g)	k_1(min^{-1})	R^2	q_e(mg/g)	k_2(g/mg/min)	R^2	kid(mg/g/$min^{1/2}$)	C	R^2
5.86007	0.05679	0.96035	0.81909	8.98393	0.99923	3.55219	9.98494	0.90139

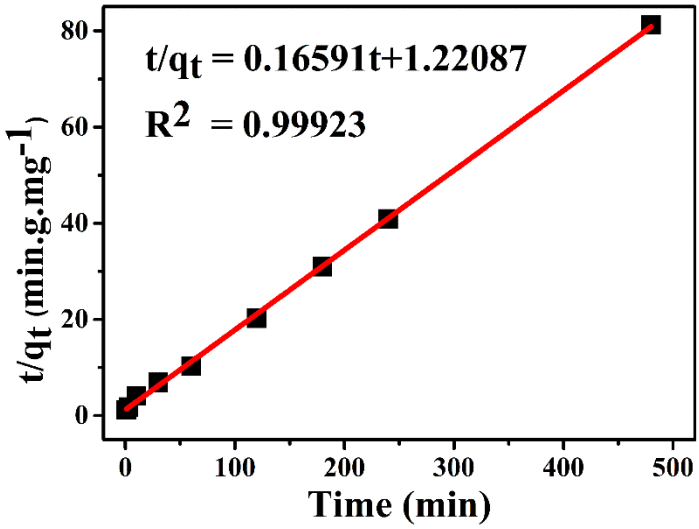

Figure S4. Pseudo-second-order model for Sr^{2+} uptake by **SZ-6**.

S6. The isotherm studies

The data of uptake amounts of Sr^{2+} were used for the determination of Sr^{2+} sorption isotherm. The adsorption capacity is defined by the value of q_e, which can be calculated from the linear equation:

$$q_e = \frac{(C_0 - C_e)V}{m}$$

Here, C_0 and C_e (mg/L) are the initial and equilibrium concentrations, respectively. V (L) is the volume of the solution and m (g) is the mass of the sample used in the experiment.

Langmuir and Freundlich isotherm models were used to analyse the mechanism of the adsorption of Sr^{2+}. The Langmuir isotherm model is hypothesized that the sorption is monolayer sorption and all the adsorption sites are equivalent. It is also based on the assumption that the energy of the adsorption is constant and the state of the exchanged ions in the structure is definite. The linear equation of the Langmuir isotherm model is expressed as follows,[5]

$$\frac{C_e}{q_e} = \frac{1}{q_m K_L} + \frac{C_e}{q_m}$$

where q_m (mg/g) is the maximum adsorption capacity at equilibrium indirectly related to complete monolayer coverage and K_L is a constant corresponding to the capacity and energy of sorption, which defines the affinity of the adsorbate with the adsorbent. Meanwhile, q_e (mg/g) is the quantity of ions adsorbed onto per unit adsorbent at different initial concentrations.

The Freundlich equation is an empirical equation based on sorption on a heterogeneous surface. The linear form of Freundlich equation can be expressed as:

$$\ln q_e = \ln K_F + \frac{1}{n} \ln C_e$$

Here, K_F and n are the Freundlich constants. K_F is related to the sorption capacity and n represents the sorption intensity, which can account for the degree of dependence of sorption on the equilibrium concentration. Values of K_F and n are calculated from the fitting result of the intercept and the slope of the plot.

Table S3. Adsorption isotherm parameters for Sr^{2+}

pH	Langmuir			Freundlich		
	q_m	K_L	R^2	K_F	n	R^2
2	11.23328	0.00378	0.98352	0.07731	1.25966	0.97458
4	59.18037	0.30653	0.99212	20.62886	4.93169	0.84232
6	59.68225	0.45475	0.9948	23.62662	5.68941	0.83523
8	58.74915	0.66047	0.99423	24.8169	5.8593	0.80336
10	61.40303	0.49992	0.98874	23.65797	5.28281	0.80551
12	46.60726	0.15825	0.98224	13.20375	4.38252	0.91316

Table S4. The Sr^{2+} uptake capacity for different sorbent materials.

Compound	Experimental conditions	q (mg/g)	Ref
Zeolite A	298 K; 1 g/L; pH=6	69.78	[3]
CST	295 K; 0.6 g/L; pH=7	33.9	[6]
MST	298 K; 1 g/L; pH=6	69.78	[7]
Iron oxide	~303 K; 5 g/L; pH=10.5	38.5	[8]
FJSM-SnS	290 K; 1 g/L; pH~7	65.2	[9]
KMS-1	1 g/L	77	[10]
KMS-2	298 K; 1 g/L; pH=6.9	86.89	[11]
GO-HAP	298 K; 0.5 g/L; pH=7.0±0.1	702.18	[12]
SZ-4	298 K; 1 g/L; pH=4	117.9	[13]
SZ-6	**298 K; 0.5 g/L; pH=10**	**61.4**	**This work**

S7. FT-IR spectra of SZ-6 before and after Sr^{2+} adsorption.

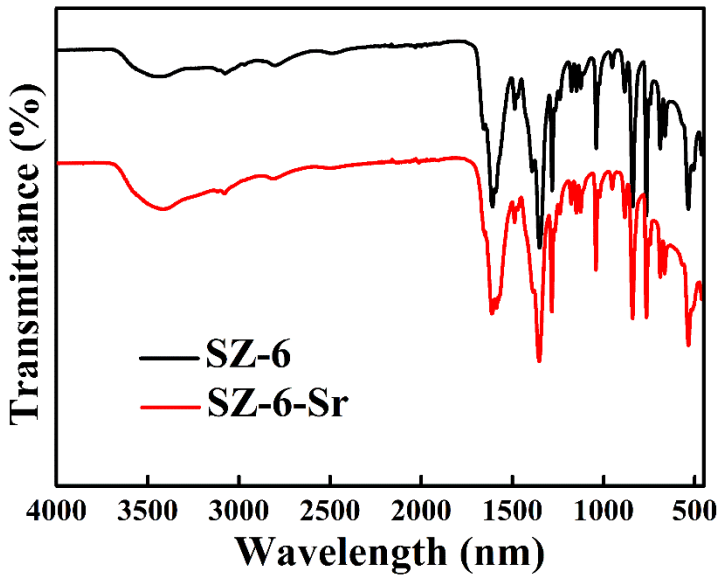

Figure S5. FT-IR spectra of **SZ-6** before and after Sr^{2+} adsorption.

S8. EDS analysis

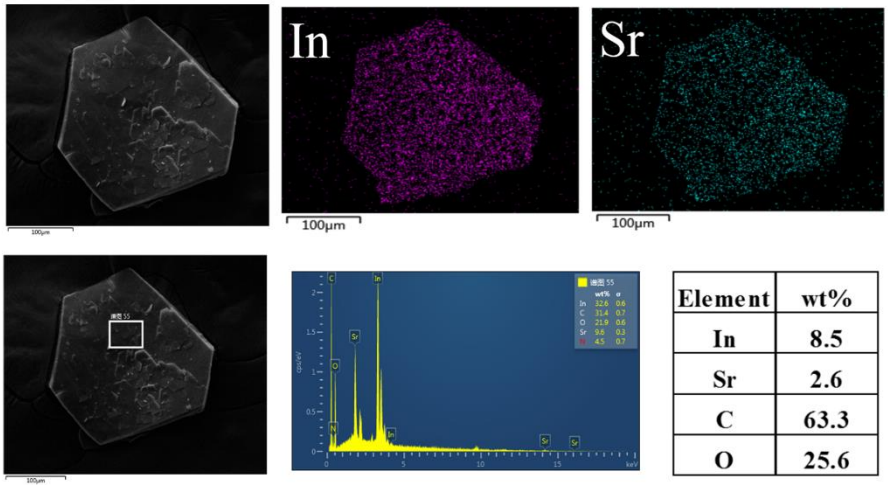

Element	wt%
In	8.5
Sr	2.6
C	63.3
O	25.6

Figure S6. EDS mapping profiles of Sr^{2+} loaded **SZ-6**

S9. X-ray photoelectron spectroscopy

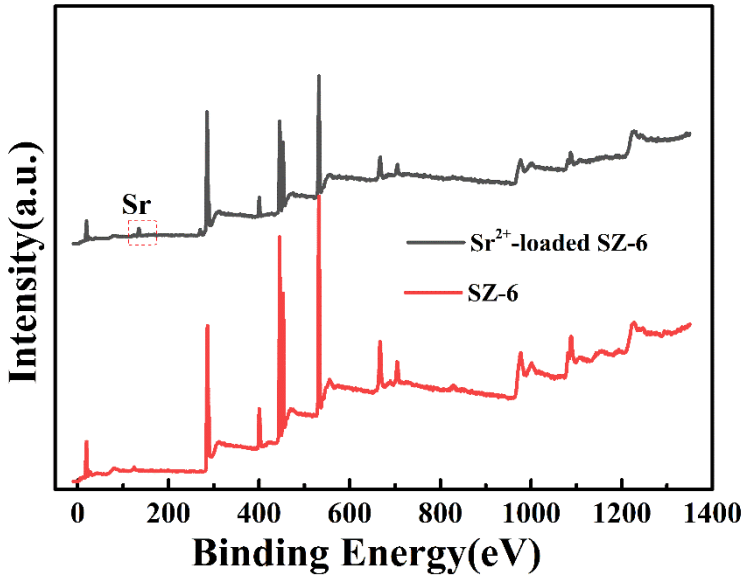

Figure S7. The full XPS spectrum of **SZ-6** and Sr^{2+}-loaded **SZ-6**

S10. The reusability test

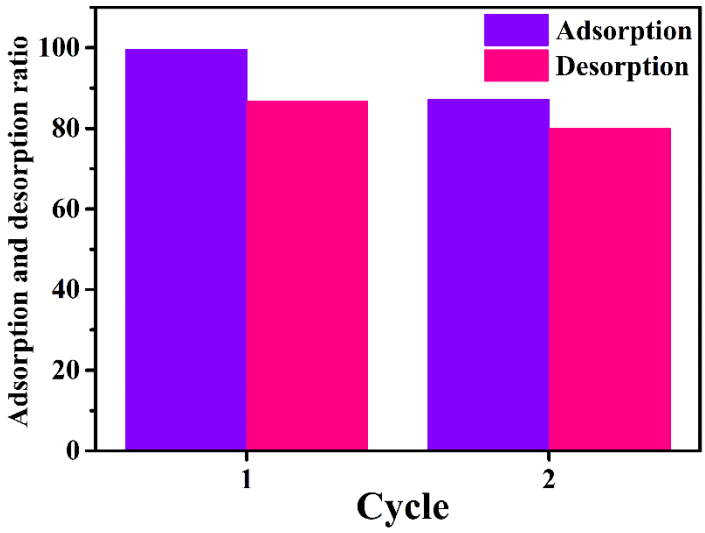

Figure S8. Adsorption and desorption ratios for two rounds.

S11. The distribution coefficient K_d

The distribution coefficient K_d is a measurement of affinity and selectivity, and is described by the follow equation:

$$K_d = \frac{V}{m}\frac{(C_0 - C_e)}{C_e}$$

where C_0 and C_e represent the initial and equilibrium concentrations of Sr^{2+}(mg/L), respectively. V is the volume (mL) of solution, and m is the mass (g) of the samples used in the experiments.

S12. Thermodynamic Study

Table S5. The Langmuir and Freundlich models fitting for Sr^{2+} sorption on SZ-6 at different temperatures.

T (K)	Langmuir			Freundlich		
	q_m	K_L	R^2	K_F	n	R^2
298	54.17662	0.37962	0.99224	20.90271	5.54234	0.8516
308	62.49231	0.42467	0.96631	21.06387	4.86189	0.92524
318	63.01488	0.39757	0.95184	20.28236	4.55794	0.92382

Table S6. The thermodynamic parameters for Sr^{2+} sorption onto **SZ-6**

T (K)	ΔG (kJ/mol)	ΔS (kJ/(mol·K)	ΔH (kJ/mol)
298	-21.643		
308	-23.331	0.1118	11.482
318	-23.879		

S13. The main components of seawater.

Table S7. The main components of seawater[12]

Component	Concentration (mol/L)
Chlorine	0.546
Sodium	0.469
Magnesium	0.0528
Sulfur	0.0282
Calcium	0.0103
Potassium	0.0102
Bromine	0.000844

Notes and references

1. G. M. Sheldrick, *Acta Crystallogr C Struct Chem*, 2015, **71**, 3-8.
2. R. Bandyopadhyay, J. Selbo, G. E. Amidon and M. Hawley, *Journal of Pharmaceutical Sciences*, 2005, **94**, 2520-2530.
3. H. Faghihian, M. Moayed, A. Firooz and M. Iravani, *Cr Chim*, 2014, **17**, 108-117.
4. H. Faghihian, M. Iravani, M. Moayed and M. Ghannadi-Maragheh, *Chem Eng J*, 2013, **222**, 41-48.
5. I. Langmuir, *J Am Chem Soc*, 1918, **40**, 1361-1403.
6. N. A. Weerasekara, K. H. Choo and S. J. Choi, *J Membrane Sci*, 2013, **447**, 87-95.
7. J. Lehto and A. Clearfield, *J Radioanal Nucl Ch*, 1987, **118**, 1-13.
8. C.-H. Liu, Y.-J. Shih, Y.-H. Huang and C.-P. Huang, *Journal of the Taiwan Institute of Chemical Engineers*, 2014, **45**, 914-920.
9. X.-H. Qi, K.-Z. Du, M.-L. Feng, J.-R. Li, C.-F. Du, B. Zhang and X.-Y. Huang, *J Mater Chem A*, 2015, **3**, 5665-5673.
10. M. J. Manos, N. Ding and M. G. Kanatzidis, *P Natl Acad Sci USA*, 2008, **105**, 3696-3699.

11. J. L. Mertz, Z. H. Fard, C. D. Malliakas, M. J. Manos and M. G. Kanatzidis, *Chem Mater*, 2013, **25**, 2116-2127.
12. T. Wen, X. L. Wu, M. C. Liu, Z. H. Xing, X. K. Wang and A. W. Xu, *Dalton T*, 2014, **43**, 7464-7472.
13. J. R. Zhang, L. H. Chen, X. Dai, L. Zhu, C. L. Xiao, L. Xu, Z. Y. Zhang, E. V. Alekseev, Y. X. Wang, C. Zhang, H. W. Zhang, Y. L. Wang, J. Diwu, Z. F. Chai and S. Wang, *Chem-Us*, 2019, **5**, 977-994.
14. Dickson, A.G., Goyet, C. (1994). Handbook of methods for the analysis of the various parameters of the carbon dioxide system in sea water. DOE report, 2, ORNL/CDIAC-74.